SUPPLEMENTARY INFORMATION

SUPPLEMENTARY FIGURE 1

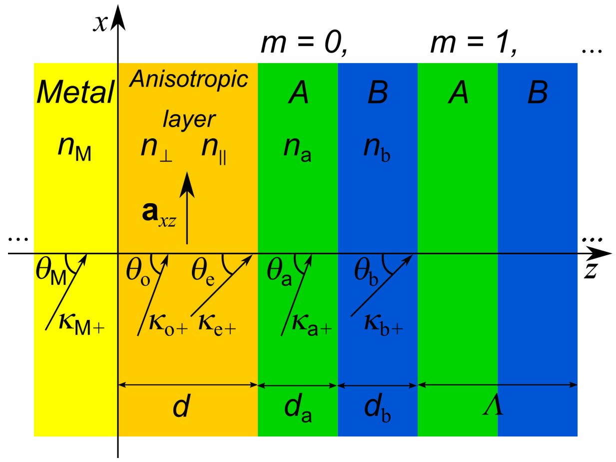

Supplementary Figure 1. Layered structure. Anisotropic layer conjugated with 1D photonic crystal (PhC) and semi-infinite metal layer with refractive index n_M. PhC consists of alternating layers A and B with thicknesses and refractive indices d_a, n_a and d_b, n_b respectively. The period of the PhC is $\Lambda = d_\mathrm{a} + d_\mathrm{b}$; m is number of unit cell. Optical properties of the anisotropic layer with thickness d are defined by refractive indices $n_\perp$, $n_\parallel$, and component $\mathbf{a}_{xz}$ of anisotropy axis unit vector along light incident plane xz. The unit vector $\boldsymbol{\kappa}$ denotes direction of light wave propagation in each layer, which is defined by angle θ.

SUPPLEMENTARY FIGURE 2

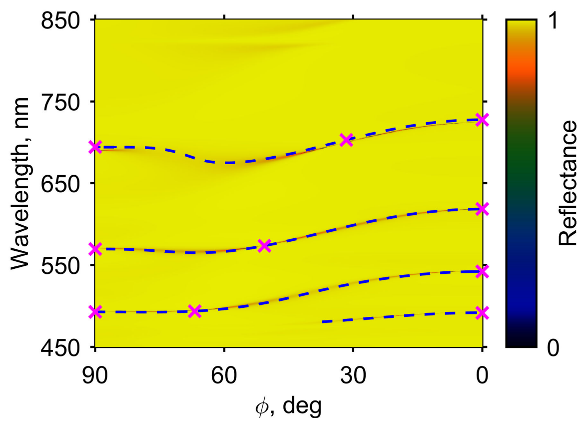

Supplementary Figure 2. Numerical transverse magnetic (TM)-polarized reflectance spectra vs anisotropy axis rotation angle ϕ for structure depicted in Supplementary Figure 1 with low loss metal (refractive index $n_\mathrm{M} = 0.14 + 20i$). Magenta crosses correspond to the asymmetric (with respect to anisotropic defect layer/metal boundary) analytical solutions for bound states in the continuum (eqs. 78 and 79). The blue dashed line shows the analytical dispersion curve for the transverse electric (TE)-polarized microcavity mode (eq. 63).

SUPPLEMENTARY FIGURE 3

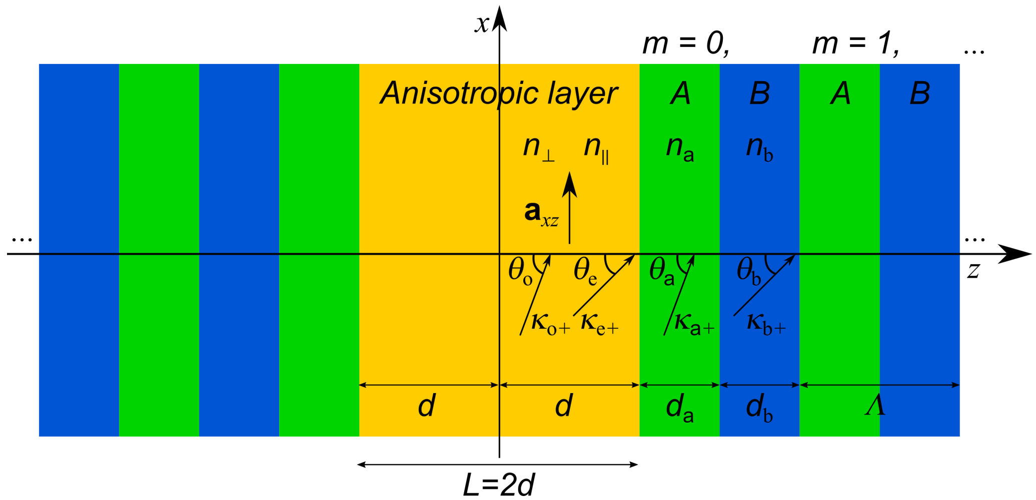

Supplementary Figure 3. Layered structure. Anisotropic layer conjugated with two 1D photonic crystals (PhC). PhC consists of alternating layers A and B with thicknesses and refractive indices d_{a}, n_{a} and d_{b}, n_{b} respectively. The period of the PhC is $\Lambda = d_{\mathrm{a}} + d_{\mathrm{b}}$; m is number of unit cell. Optical properties of the anisotropic layer with thickness $L = 2d$ are defined by refractive indices $n_\perp$, $n_\parallel$, and component $\mathbf{a}_{xz}$ of anisotropy axis unit vector along light incident plane xz. The unit vector $\boldsymbol{\kappa}$ denotes direction of light wave propagation in each layer, which is defined by angle θ.

SUPPLEMENTARY FIGURE 4

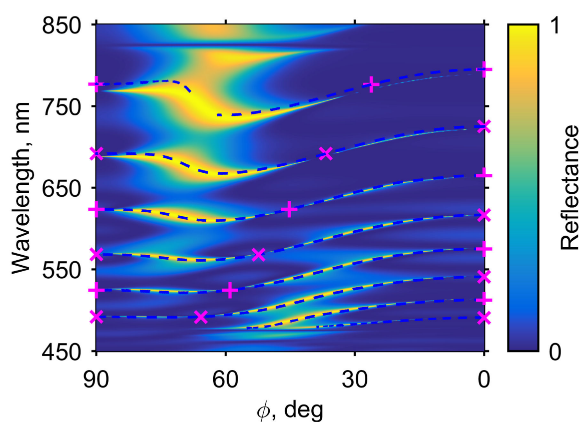

Supplementary Figure 4. Numerical transverse magnetic (TM)-polarized reflectance spectra vs anisotropy axis rotation angle ϕ for structure depicted in Supplementary Figure 3. Magenta pluses correspond to the symmetric (with respect to the center of the anisotropic defect layer) analytical solutions for bound states in the continuum, crosses correspond to the asymmetric solutions (eqs. 78, 79). The blue dashed line shows the analytical dispersion curve for the transverse electric (TE)-polarized microcavity mode (eq. 63).

SUPPLEMENTARY FIGURE 5

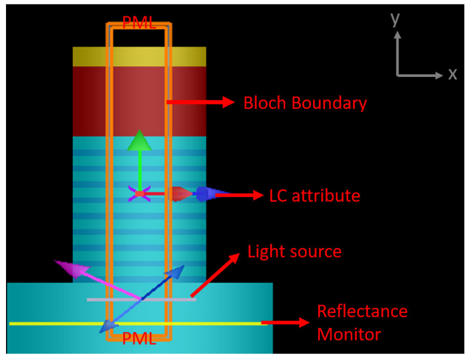

Supplementary Figure 5. The schematic diagram of Finite-Difference Time-Domain simulation.

SUPPLEMENTARY FIGURE 6

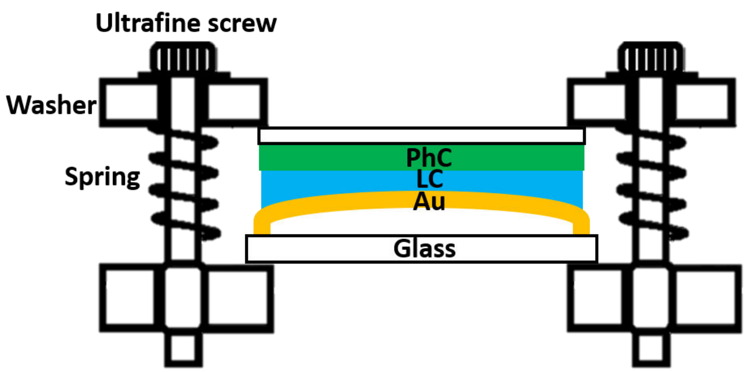

Supplementary Figure 6. The schematic diagram of experimental measured sample. Liquid crystal (LC) layer conjugated with 1D photonic crystal (PhC) and gold film (Au).

SUPPLEMENTARY FIGURE 7

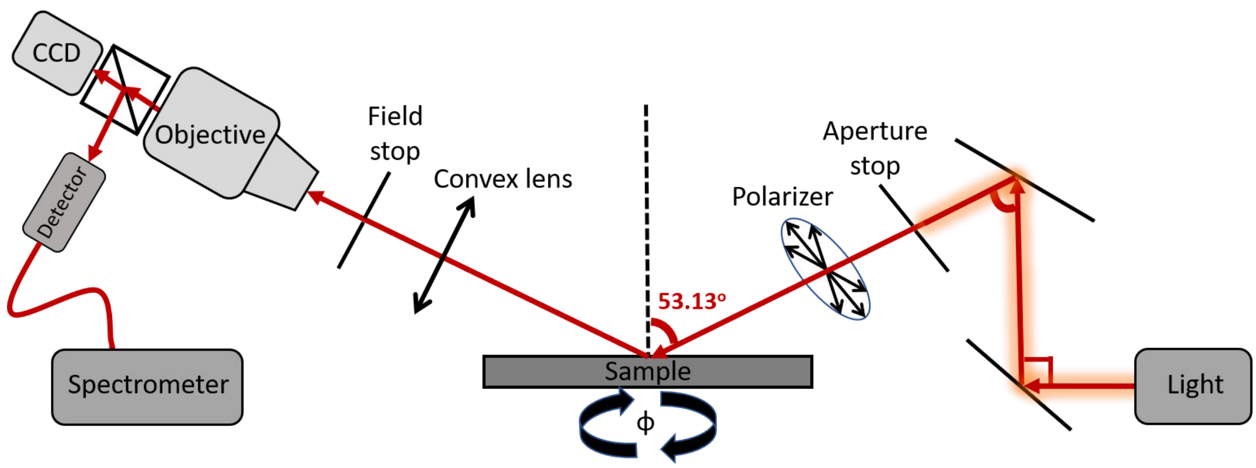

Supplementary Figure 7. The schematic diagram of experimental setup to measure reflectance and transmittance spectra by rotating the sample as azimuthal angle ϕ. Charge-coupled device (CCD).

SUPPLEMENTARY FIGURE 8

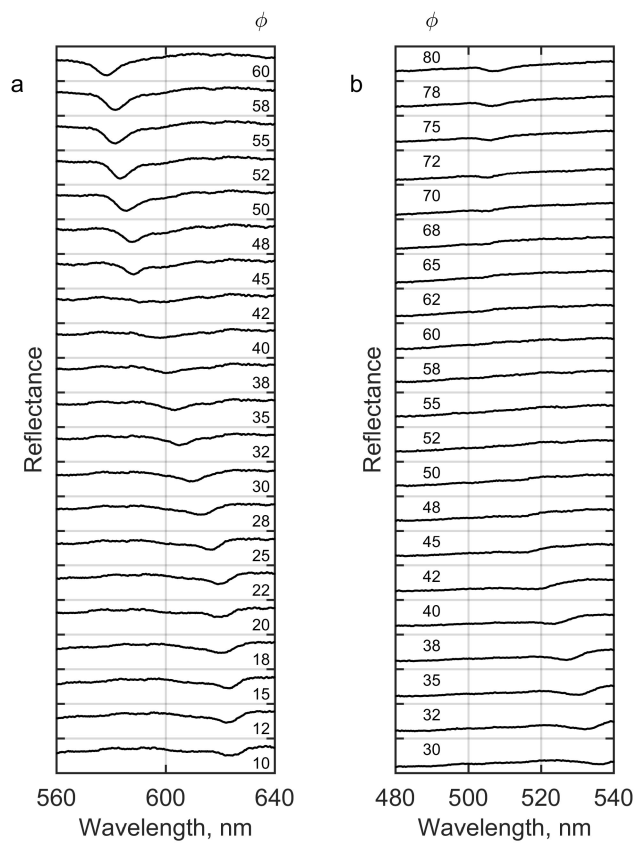

Supplementary Figure 8. Experimental spectra in a vicinity of the Friedrich-Wintgen bound states in the continuum.

SUPPLEMENTARY FIGURE 9

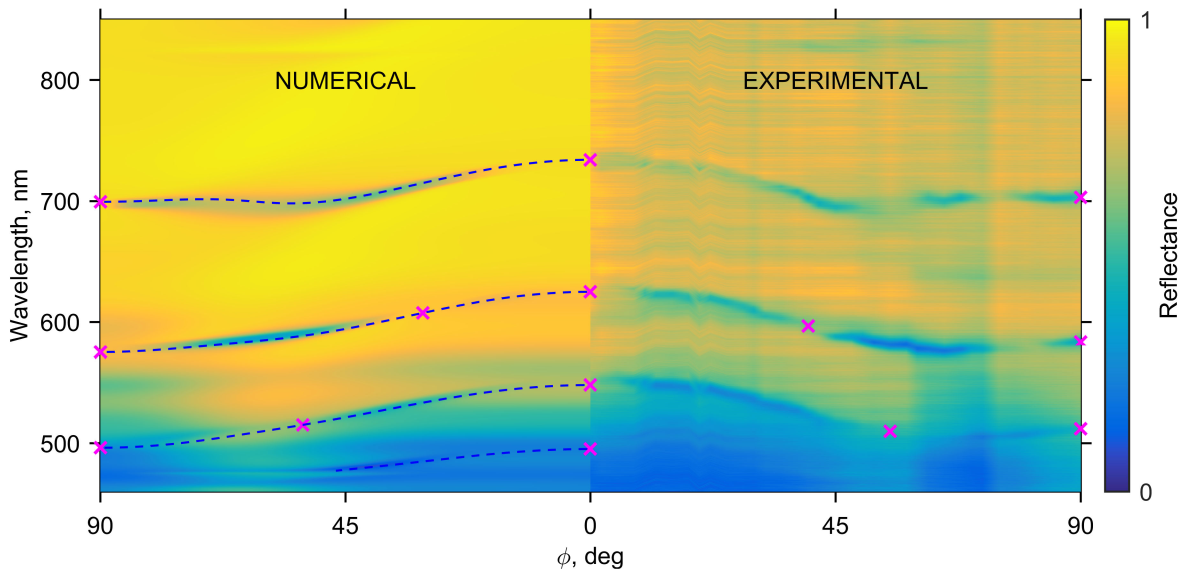

Supplementary Figure 9. Experimental (right panel) and numerical (left panel) transverse magnetic (TM)-polarized reflectance spectra vs liquid crystal anisotropy axis rotation angle ϕ. Magenta crosses mark the asymmetric analytical solutions for bound states in the continuum (eqs. 78 and 79) and experimental points of Fano resonance collapse. The blue dashed line shows the analytical dispersion curve for the transverse electric (TE)-polarized microcavity mode (eq. 63).

SUPPLEMENTARY FIGURE 10

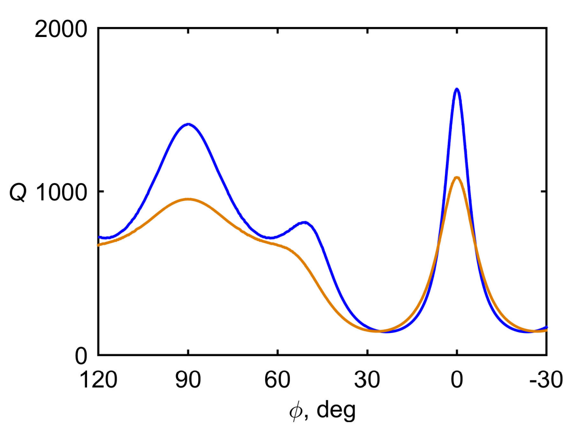

Supplementary Figure 10. The analytical quality (Q) factor (eq. 76) one of the resonance curves in Supplementary Figure 9 with the Friedrich-Wintgen bound state in the continuum ($\phi = 40°$, $\lambda = 596.6$ nm) for experimental case ($n_{\mathrm{M}}(596.6\mathrm{nm}) = 0.14 + 3.697i$, orange), and with low loss metal ($n_{\mathrm{M}}(596.6\mathrm{nm}) = 0.14 + 4.697i$, blue).

SUPPLEMENTARY NOTE 1. SPIN MODEL

Let us write the Schrödinger equation for the toy model of electron in magnetic field (see Fig.1 (main article)):

$$\left[\frac{1}{2m}(i\hbar\nabla + e\mathbf{A})^2 + U_0(z) - \boldsymbol{\sigma}\mathbf{B}(z) - E\right]\Psi = 0. \tag{1}$$

The orbital motion has characteristic length $a_B^2 = \frac{\hbar c}{eB}$ which in the magnetic field of $10^3 Oe$ equals 100 nm. Then for layer of thickness $L \ll a_B$ we can disregard the orbital contribution in eq. (1) and rewrite as follows

$$\left[\nabla^2 - U_0(z) + (\boldsymbol{\sigma}\mathbf{B}(z)) + E\right]\Psi = 0. \tag{2}$$

Next we substitute the step-wise magnetic filed as shown in Fig.1 (main article). Then Hamiltonian (2) will take the following form

$$\widehat{H} = \begin{cases} -\frac{d^2}{dz^2} - \sigma_x B & \text{if } |z| > L/2; \\ -\frac{d^2}{dz^2} + U_0 - \sigma_x B\cos(\phi) - \sigma_z B\sin(\phi) & \text{if } |z| < L/2. \end{cases} \tag{3}$$

In the outer layers which form the radiation continua with the following propagating solutions

$$\Psi_{\mathbf{k}_\sigma}(z) = \exp(i\mathbf{k}_\sigma\mathbf{z})|\sigma\rangle, \tag{4}$$

where $\sigma =\uparrow,\downarrow$

$$|\uparrow\rangle = \begin{pmatrix} 1 \\ 0 \end{pmatrix}, \quad |\downarrow\rangle = \begin{pmatrix} 0 \\ 1 \end{pmatrix}, \tag{5}$$

and

$$E = k_\sigma^2 \mp B. \tag{6}$$

Respectively for the inner layer we have

$$\Psi_{\mathbf{k}s}(z) = \exp(i\mathbf{k}_s\mathbf{z})|s\rangle, \tag{7}$$

where $s = 1, 2$

$$|1\rangle = \begin{pmatrix} \cos(\phi/2) \\ \sin(\phi/2) \end{pmatrix}, \quad |2\rangle = \begin{pmatrix} -\sin(\phi/2) \\ \cos(\phi/2) \end{pmatrix}, \tag{8}$$

and

$$E = k_s^2 + U_0 \mp B. \tag{9}$$

SUPPLEMENTARY NOTE 2. SCATTERING PROBLEM

Let us choose the energy of incident electron in a way that only spin up channel is open. Then at the left ($z < -L/2$) we have

$$\Psi_L(z) = (e^{i\mathbf{k}_\uparrow \mathbf{z}} + r_\uparrow e^{-i\mathbf{k}_\uparrow \mathbf{z}})|\uparrow\rangle. \tag{10}$$

Inside the defect layer ($|z| < L/2$) both channels are open and therefore one can present the solutions as follows

$$\Psi_B(z) = \sum_{s=1,2} (a_s e^{i\mathbf{k}_s \mathbf{z}} + b_s e^{-i\mathbf{k}_s \mathbf{z}})|s\rangle. \tag{11}$$

At last at the right side ($z > L/2$) we write

$$\Psi_R(z) = t_\uparrow e^{i\mathbf{k}_\uparrow \mathbf{z}}|\uparrow\rangle. \tag{12}$$

Here $r_\uparrow$ and $t_\uparrow$ are the reflection and transmission amplitudes. Next, assume electron with spin σ incidents with wave vector $\mathbf{k}_\sigma = (k_{x\sigma}, k_{z\sigma})$ and reflecting with the reflection amplitude r_σ. Because of preservation of transverse component of moment $k_{x\sigma} = k_{xs} = k_x$ we obtain the following equations:

$$\begin{aligned}
1 + r_\uparrow &= (a_1 + b_1)\cos(\phi/2) - (a_2 + b_2)\sin(\phi/2),\\
k_{z\uparrow}(1 - r_\uparrow) &= k_{z1}(a_1 - b_1)\cos(\phi/2) - k_{z2}(a_2 - b_2)\sin(\phi/2),\\
r_\downarrow &= (a_1 + b_1)\sin(\phi/2) + (a_2 + b_2)\cos(\phi/2),\\
-k_{z\downarrow} r_\downarrow &= k_{z1}(a_1 - b_1)\sin(\phi/2) + k_{z2}(a_2 - b_2)\cos(\phi/2),\\
t_\uparrow e^{ik_{z\uparrow}L} &= (a_1 e^{ik_{z1}L} + b_1 e^{-ik_{z1}L})\cos(\phi/2) - (a_2 e^{ik_{z2}L} + b_2 e^{-ik_{z2}L})\sin(\phi/2),\\
k_{z\uparrow} t_\uparrow e^{ik_{z\uparrow}L} &= k_{z1}(a_1 e^{ik_{z1}L} - b_1 e^{-ik_{z1}L})\cos(\phi/2) - k_{z2}(a_2 e^{ik_{z2}L} - b_2 e^{-ik_{z2}L})\sin(\phi/2),\\
t_\downarrow e^{ik_{z\downarrow}L} &= (a_1 e^{ik_{z1}L} + b_1 e^{-ik_{z1}L})\sin(\phi/2) + (a_2 e^{ik_{z2}L} + b_2 e^{-ik_{z2}L})\cos(\phi/2),\\
k_{z\downarrow} t_\downarrow e^{ik_{z\downarrow}L} &= k_{z1}(a_1 e^{ik_{z1}L} - b_1 e^{-ik_{z1}L})\sin(\phi/2) + k_{z2}(a_2 e^{ik_{z2}L} - b_2 e^{-ik_{z2}L})\cos(\phi/2).
\end{aligned} \tag{13}$$

The bound state in the continuum (BIC) as the mode localized inside the layer can be found from equations of continuity at the interfaces. These equations can be simplified with account of symmetry relative to $z \to -z$. Then the symmetric (even) BIC can be written as

$$\psi_{BIC,sym}(z) = \begin{cases} a_1 \cos(k_{z1}z)|1\rangle + b_2 \cos(k_{z2}z)|2\rangle & \text{if } |z| < L/2 \\ c e^{(-|k_{z\downarrow}|z)}|\downarrow\rangle & \text{if } |z| > L/2, \end{cases} \tag{14}$$

where the last contribution is the result of evanescent mode and asymmetric BIC

$$\psi_{BIC,asym}(z) = \begin{cases} a_1 \sin(k_{z1}z)|1\rangle + b_2 \sin(k_{z2}z)|2\rangle & \text{if } |z| < L/2 \\ sign(z) c e^{(-|k_{z\downarrow}|z)}|\downarrow\rangle & \text{if } |z| > L/2. \end{cases} \tag{15}$$

We imply that the modes equal zero at the spin up continuum and obey the continuity equations for the evanescent mode spin down. As the result we obtain the following equations for the symmetric BIC

$$\begin{aligned}
a_1 \cos(\phi/2)\cos(k_{z1}L/2) - b_2 \sin(\phi/2)\cos(k_{z2}L/2) &= 0,\\
a_1 \sin(\phi/2)\cos(k_{z1}L/2) + b_2 \cos(\phi/2)\cos(k_{z2}L/2) &= c e^{(-|k_{z\downarrow}|L/2)},\\
a_1 k_{z1} \sin(\phi/2)\sin(k_{z1}L/2) + b_2 k_{z2} \cos(\phi/2)\sin(k_{z2}L/2) &= c|k_{z\downarrow}| e^{(-|k_{z\downarrow}|L/2)}.
\end{aligned} \tag{16}$$

Thus, we obtain the following equation for the symmetric BIC points

$$-\tan^2(\phi/2) = \frac{k_{z2}\tan(k_{z2}L/2) - |k_{z\downarrow}|}{k_{z1}\tan(k_{z1}L/2) - |k_{z\downarrow}|}, \tag{17}$$

and respectively for the asymmetric (odd) BIC points

$$-\tan^2(\phi/2) = \frac{k_{z2}\cot(k_{z2}L/2) + |k_{z\downarrow}|}{k_{z1}\cot(k_{z1}L/2) + |k_{z\downarrow}|}. \tag{18}$$

SUPPLEMENTARY NOTE 3. PHOTONIC MODEL

A. Description of the structure

Consider a structure consisting of an anisotropic layer with a thickness d, embedded between semi-infinite 1D photonic crystal (PhC) and metal (Supplementary Figure 1). The unit cell of PhC consists of alternating layers A and B with refractive indices (RI) and thicknesses $n_{\mathrm{a}} = \sqrt{\varepsilon_{\mathrm{a}}}$, d_{a} and $n_{\mathrm{b}} = \sqrt{\varepsilon_{\mathrm{b}}}$, d_{b}. The lattice period is $\Lambda = d_{\mathrm{a}} + d_{\mathrm{b}}$. RI of metal is $n_{\mathrm{M}} = \sqrt{\varepsilon_{\mathrm{M}}}$.

The optical properties of the anisotropic uniaxial layer are described by the dielectric permittivity tensor $\hat{\epsilon}$. This tensor can be expressed in terms of the transverse $n_{\perp} = \sqrt{\varepsilon_{\mathrm{o}}}$ and the longitudinal $n_{\|} = \sqrt{\varepsilon_{\mathrm{o}} + \varepsilon'}$ layer refractive indices. Let the direction of the optical axis be determined by the unit vector $\mathbf{a}$, then the components of the dielectric permittivity tensor are written as [1]:

$$\epsilon_{ij} = \varepsilon_{\mathrm{o}}\delta_{ij} + \varepsilon' \mathrm{a}_i \mathrm{a}_j. \tag{19}$$

Here a_i are the components of the vector $\mathbf{a}$, δ_{ij} is the Kronecker symbol. The value of ε' responses for the anisotropy magnitude. In the case of $\varepsilon' = 0$, the anisotropy disappears, and the tensor (19) reduces into a scalar and the layer has an ordinary RI $n_{\mathrm{o}} = \sqrt{\varepsilon_{\mathrm{o}}}$.

Consider the propagation in the structure of plane light waves in the form $e^{i(\mathbf{kr}-\omega t)}$, where $\mathbf{k}$ is the wave vector, ω is the circular frequency of light, $\mathbf{r}$ is the radius vector and t is the time. In each layer, we consider two mutually orthogonal types of solutions of Maxwell's equations for nonmagnetic media:

$$\begin{pmatrix} 0 & \nabla\times \\ -\nabla\times & 0 \end{pmatrix} \begin{pmatrix} \mathbf{E} \\ \mathbf{H} \end{pmatrix} = \frac{1}{c}\frac{\partial}{\partial t} \begin{pmatrix} \hat{\epsilon}\mathbf{E} \\ \mathbf{H} \end{pmatrix} = -ik_0 \begin{pmatrix} \hat{\epsilon}\mathbf{E} \\ \mathbf{H} \end{pmatrix}, \tag{20}$$

where $k_0 = \omega/c$ is the wave number in vacuum, c is the speed of light. In isotropic layers, two orthogonal solutions are determined by the plane of incidence xz. This is a transverse-electric wave (TE-wave), having the components E_y, H_x, H_z, and a transverse-magnetic wave (TM-wave), having the components H_y, E_x, E_z. In the anisotropic layer, two orthogonal types of solution are determined by the direction of the optical axis $\mathbf{a}$. This is an extraordinary wave (e-wave), for which $(\mathbf{E}_{\mathrm{e}}\mathbf{a}) \neq 0$, and an ordinary wave (o-wave), for which $(\mathbf{E}_{\mathrm{o}}\mathbf{a}) = 0$. When a plane wave propagates in a layered medium, the projection of the wave vector parallel to the interfaces $k_{\|} = k_x$ has a constant value in all layers. In further calculations, we omit the factor $e^{i(k_x x - \omega t)}$ that is common to all field vectors. The system (20) gives us the wave equation in the Helmholtz form analogous to (2):

$$\left[\nabla^2 + \epsilon_{ij}(z)k_0^2\right]\psi = 0, \; \psi = E_y, H_y. \tag{21}$$

B. TE-waves

The general solution of the wave equation (21) in each layer is written as the sum of the forward "+" and the backward "−" waves propagating along and opposite (backwards) to the z axis, respectively. The TE-wave field in the layer A, with the cell number m $(d + m\Lambda \leq z < d + m\Lambda + d_{\mathrm{a}})$, is written as:

$$E_{\mathrm{a}y}^{(m)} = e^{iK\Lambda m}(A_+ e^{ik_{\mathrm{a}z}(z-(d+m\Lambda))} + A_- e^{-ik_{\mathrm{a}z}(z-(d+m\Lambda))}); \tag{22}$$

$$H_{\mathrm{a}x}^{(m)} = \frac{k_{\mathrm{a}z}}{k_0} e^{iK\Lambda m}(-A_+ e^{ik_{\mathrm{a}z}(z-(d+m\Lambda))} + A_- e^{-ik_{\mathrm{a}z}(z-(d+m\Lambda))}). \tag{23}$$

In the layer B, with the cell number m $(d + m\Lambda + d_{\mathrm{a}} \leq z < d + (m+1)\Lambda)$:

$$E_{\mathrm{b}y}^{(m)} = e^{iK\Lambda m}(B_+ e^{ik_{\mathrm{b}z}(z-(d+m\Lambda+d_{\mathrm{a}}))} + B_- e^{-ik_{\mathrm{b}z}(z-(d+m\Lambda+d_{\mathrm{a}}))}); \tag{24}$$

$$H_{\mathrm{b}x}^{(m)} = \frac{k_{\mathrm{b}z}}{k_0} e^{iK\Lambda m}(-B_+ e^{ik_{\mathrm{b}z}(z-(d+m\Lambda+d_{\mathrm{a}}))} + B_- e^{-ik_{\mathrm{b}z}(z-(d+m\Lambda+d_{\mathrm{a}}))}), \tag{25}$$

where A_+, A_-, B_+, B_- are amplitudes, and the factor $e^{iK\Lambda m}$ arises owing to Bragg diffraction and is a consequence of the periodicity of the structure [2, 3], $m = 0, 1, 2, ...$, K is the Bloch wave number. The projection of the wave vector on the z axis is defined as:

$$k_{jz} = \sqrt{k_0^2\varepsilon_j - k_x^2}, \; j = \mathrm{a,b}. \tag{26}$$

Let us use the continuity condition for the tangential field components and perform the matching of the equations (22) - (25) on the boundary between the B layer in the $(m-1)$-th cell and the A layer in m-th cell (for $z = d + m\Lambda$), as well as on the boundary between layers A and B in the m-th cell (for $z = d + m\Lambda + d_\mathrm{a}$). This gives us a system of four equations for four unknowns: A_+, A_-, B_+, B_-. After excluding B_+, B_-, this system is written in the following form:

$$\begin{cases} A_+(e^{ik_{\mathrm{a}z}d_\mathrm{a}} - e^{iK\Lambda}e^{-ik_{\mathrm{b}z}d_\mathrm{b}}) - A_- r_{\mathrm{ab}\perp}(e^{-ik_{\mathrm{a}z}d_\mathrm{a}} - e^{iK\Lambda}e^{-ik_{\mathrm{b}z}d_\mathrm{b}}) = 0, \\ -A_+ r_{\mathrm{ab}\perp}(e^{ik_{\mathrm{a}z}d_\mathrm{a}} - e^{iK\Lambda}e^{ik_{\mathrm{b}z}d_\mathrm{b}}) + A_-(e^{-ik_{\mathrm{a}z}d_\mathrm{a}} - e^{iK\Lambda}e^{ik_{\mathrm{b}z}d_\mathrm{b}}) = 0, \end{cases} \tag{27}$$

where the Fresnel reflection coefficient for the TE-wave is written as:

$$r_{\mathrm{ab}\perp} = \frac{k_{\mathrm{a}z} - k_{\mathrm{b}z}}{k_{\mathrm{a}z} + k_{\mathrm{b}z}}. \tag{28}$$

By equating the determinant (27) to zero, we obtain the dispersion equation for bulk TE-waves in PhC – the Rytov equation [2–6]:

$$\cos(K\Lambda) = \cos(k_{\mathrm{a}z}d_\mathrm{a})\cos(k_{\mathrm{b}z}d_\mathrm{b}) - \frac{1 + r_{\mathrm{ab}\perp}^2}{1 - r_{\mathrm{ab}\perp}^2}\sin(k_{\mathrm{a}z}d_\mathrm{a})\sin(k_{\mathrm{b}z}d_\mathrm{b}). \tag{29}$$

Eq. (29) defines the band structure $\omega(K, k_x)$ for PhC. The condition $|\cos(K\Lambda)| < 1$ corresponds to real K and, therefore, bands with propagating light. In the opposite case of $|\cos(K\Lambda)| > 1$, the Bloch wave number is complex, and the corresponding frequencies form a photonic bandgap, with boundaries determined by the condition $|\cos(K\Lambda)| = 1$.

C. TM-waves

Similarly, let us write the TM-wave field in the A layer, with the cell number m $(d + m\Lambda \leq z < d + m\Lambda + d_\mathrm{a})$:

$$E_{\mathrm{a}x}^{(m)} = e^{iK\Lambda m}(A'_+ e^{ik_{\mathrm{a}z}(z-(d+m\Lambda))} - A'_- e^{-ik_{\mathrm{a}z}(z-(d+m\Lambda))}); \tag{30}$$

$$H_{\mathrm{a}y}^{(m)} = \frac{k_0\varepsilon_\mathrm{a}}{k_{\mathrm{a}z}} e^{iK\Lambda m}(A'_+ e^{ik_{\mathrm{a}z}(z-(d+m\Lambda))} + A'_- e^{-ik_{\mathrm{a}z}(z-(d+m\Lambda))}). \tag{31}$$

In the B layer with the cell number m $(d + m\Lambda + d_\mathrm{a} \leq z < d + (m+1)\Lambda)$:

$$E_{\mathrm{b}x}^{(m)} = e^{iK\Lambda m}(B'_+ e^{ik_{\mathrm{b}z}(z-(d+m\Lambda+d_\mathrm{a}))} - B'_- e^{-ik_{\mathrm{b}z}(z-(d+m\Lambda+d_\mathrm{a}))}); \tag{32}$$

$$H_{\mathrm{b}y}^{(m)} = \frac{k_0\varepsilon_\mathrm{b}}{k_{\mathrm{b}z}} e^{iK\Lambda m}(B'_+ e^{ik_{\mathrm{b}z}(z-(d+m\Lambda+d_\mathrm{a}))} + B'_- e^{-ik_{\mathrm{b}z}(z-(d+m\Lambda+d_\mathrm{a}))}), \tag{33}$$

where A'_+, A'_-, B'_+, B'_- are amplitudes. Performing the same matching at the boundaries between the layers as for TE-wave, we obtain the dispersion equation for bulk TM-waves, which is obtained from (29) by replacing $r_{\mathrm{ab}\perp}$ with the Fresnel reflection coefficient for TM-wave:

$$r_{\mathrm{ab}\parallel} = \frac{\varepsilon_\mathrm{b}k_{\mathrm{a}z} - \varepsilon_\mathrm{a}k_{\mathrm{b}z}}{\varepsilon_\mathrm{a}k_{\mathrm{b}z} + \varepsilon_\mathrm{b}k_{\mathrm{a}z}}. \tag{34}$$

SUPPLEMENTARY NOTE 4. DISPERSION EQUATIONS

A. Fields in anisotropic layer

Consider the propagation of light in the structure at the Brewster's angle for the PhC lattice: $\theta_{\rm a}+\theta_{\rm b}=\pi/2$, where $\theta_{\rm a}=\arctan\left(n_{\rm b}/n_{\rm a}\right)$. To describe the propagation in the anisotropic layer we apply the convenient analytical method proposed in [7]. Let us write the Cartesian coordinates of the vector $\mathbf{a}$ assuming that it lies in the xy plane:

$$\mathbf{a}=(\sin{(\phi)},\cos{(\phi)},0), \tag{35}$$

where ϕ is the angle between the direction $\mathbf{a}$ and the y axis. The direction of the optical axis $\mathbf{a}$ and the relative anisotropy $\eta=\varepsilon'/\varepsilon_{\rm o}$ determine the direction and length of the wave vector for e-wave:

$$\theta_{\rm e}=\arctan\left(\frac{k_x}{k_{\rm e\mathit{z}}}\right)=\arctan\left(\frac{k_x}{\sqrt{\varepsilon_{\rm o}k_0^2(1+\eta)-k_x^2(1+\eta\sin^2{(\phi)})}}\right); \tag{36}$$

$$k_{\rm e}=k_0n_{\rm e}=k_0\sqrt{\varepsilon_{\rm e}},\ \varepsilon_{\rm e}=\frac{\varepsilon_{\rm o}(1+\eta)}{1+\eta\sin^2{(\phi)}\sin^2{(\theta_{\rm e})}}. \tag{37}$$

The direction and length of the wave vector for the o-wave does not depend on direction of the optical axis:

$$\theta_{\rm o}=\arctan\left(\frac{k_x}{k_{\rm o\mathit{z}}}\right)=\arctan\left(\frac{k_x}{\sqrt{\varepsilon_{\rm o}k_0^2-k_x^2}}\right),\ k_{\rm o}=k_0n_{\rm o}. \tag{38}$$

A unit vector along the direction of propagation is defined as shown in Supplementary Figure 1:

$$\boldsymbol{\kappa}_{j+,-}=\mathbf{k}_{j+,-}/k_j=(\sin{(\theta_j)},0,\pm\cos{(\theta_j)}),\ j=\text{e,o}. \tag{39}$$

At certain direction of the optical axis $\mathbf{a}$ and the direction of propagation of the e- and o-waves $\boldsymbol{\kappa}_{j+,-}$ we find the directions of the vectors of the electromagnetic field. For e-wave:

$$\mathbf{E}_{\rm e+,-}=E_{\rm e+,-}\left(\mathbf{a}-\boldsymbol{\kappa}_{\rm e+,-}(\mathbf{a}\boldsymbol{\kappa}_{\rm e+,-})\frac{\varepsilon_{\rm e}}{\varepsilon_{\rm o}}\right), \tag{40}$$

$$\mathbf{H}_{\rm e+,-}=\frac{k_{\rm e}}{k_0}\left[\boldsymbol{\kappa}_{\rm e+,-}\times\mathbf{E}_{\rm e+,-}\right]. \tag{41}$$

For the o-wave we have

$$\mathbf{E}_{\rm o+,-}=E_{\rm o+,-}\left[\mathbf{a}\times\boldsymbol{\kappa}_{\rm o+,-}\right], \tag{42}$$

$$\mathbf{H}_{\rm o+,-}=\frac{k_{\rm o}}{k_0}\left[\boldsymbol{\kappa}_{\rm o+,-}\times\mathbf{E}_{\rm o+,-}\right], \tag{43}$$

where $E_{\rm e+,-},E_{\rm o+,-}$ are amplitudes. The general solution of the system (20) in the anisotropic layer is written as sum of the forward and backward waves ($0\le z<d$):

$$\mathbf{E}_{\rm e,o}=\mathbf{E}_{\rm e,o+}e^{ik_{{\rm e,o}z}z}+\mathbf{E}_{\rm e,o-}e^{-ik_{{\rm e,o}z}z}, \tag{44}$$

$$\mathbf{H}_{\rm e,o}=\mathbf{H}_{\rm e,o+}e^{ik_{{\rm e,o}z}z}+\mathbf{H}_{\rm e,o-}e^{-ik_{{\rm e,o}z}z}. \tag{45}$$

Using (35), (39) - (45), we write the tangential components for e-wave as:

$$E_{{\rm e}x}=(E_{\rm e+}e^{ik_{{\rm e}z}z}+E_{\rm e-}e^{-ik_{{\rm e}z}z})\left(1-\frac{\varepsilon_{\rm e}}{\varepsilon_{\rm o}}\sin^2{(\theta_{\rm e})}\right)\sin{(\phi)}, \tag{46}$$

$$E_{\mathrm{e}y} = (E_{\mathrm{e}+}e^{ik_{\mathrm{e}z}z} + E_{\mathrm{e}-}e^{-ik_{\mathrm{e}z}z})\cos{(\phi)}, \tag{47}$$

$$H_{\mathrm{e}x} = \frac{k_{\mathrm{e}}}{k_0}(-E_{\mathrm{e}+}e^{ik_{\mathrm{e}z}z} + E_{\mathrm{e}-}e^{-ik_{\mathrm{e}z}z})\cos{(\theta_{\mathrm{e}})}\cos{(\phi)}, \tag{48}$$

$$H_{\mathrm{e}y} = \frac{k_{\mathrm{e}}}{k_0}(E_{\mathrm{e}+}e^{ik_{\mathrm{e}z}z} - E_{\mathrm{e}-}e^{-ik_{\mathrm{e}z}z})\cos{(\theta_{\mathrm{e}})}\sin{(\phi)}, \tag{49}$$

and tangential components for the o-wave are:

$$E_{\mathrm{o}x} = (E_{\mathrm{o}+}e^{ik_{\mathrm{o}z}z} - E_{\mathrm{o}-}e^{-ik_{\mathrm{o}z}z})\cos{(\theta_{\mathrm{o}})}\cos{(\phi)}, \tag{50}$$

$$E_{\mathrm{o}y} = (-E_{\mathrm{o}+}e^{ik_{\mathrm{o}z}z} + E_{\mathrm{o}-}e^{-ik_{\mathrm{o}z}z})\cos{(\theta_{\mathrm{o}})}\sin{(\phi)}, \tag{51}$$

$$H_{\mathrm{o}x} = \frac{k_{\mathrm{o}}}{k_0}(E_{\mathrm{o}+}e^{ik_{\mathrm{o}z}z} + E_{\mathrm{o}-}e^{-ik_{\mathrm{o}z}z})\cos^2{(\theta_{\mathrm{o}})}\sin{(\phi)}, \tag{52}$$

$$H_{\mathrm{o}y} = \frac{k_{\mathrm{o}}}{k_0}(E_{\mathrm{o}+}e^{ik_{\mathrm{o}z}z} + E_{\mathrm{o}-}e^{-ik_{\mathrm{o}z}z})\cos{(\phi)}. \tag{53}$$

B. Solution for localized and propagating modes

The anisotropic layer serves as a microcavity embedded between two mirrors, metallic from one side and multilayer PhC structure from the other for the frequency in the bandgap. Matching the fields (46) - (53) to the decaying solutions in the mirrors yields the solutions for the whole structure. An isotropic semi-infinite metal mirror is opaque to waves of any polarization – light is partially reflected from its surface and partially absorbed ($Im(n_{\mathrm{M}}) > 0$) inside its bulk. We write the TE-wave field in the metal for $z < 0$ as follows

$$E_{\mathrm{M}y} = M_{-}e^{-ik_{\mathrm{M}z}z}; \tag{54}$$

$$H_{\mathrm{M}x} = \frac{k_{\mathrm{M}z}}{k_0}M_{-}e^{-ik_{\mathrm{M}z}z}. \tag{55}$$

Similarly, the TM-wave field in the metal for $z < 0$ is:

$$E_{\mathrm{M}x} = -M'_{-}e^{-ik_{\mathrm{M}z}z}; \tag{56}$$

$$H_{\mathrm{M}y} = \frac{k_0\varepsilon_{\mathrm{M}}}{k_{\mathrm{M}z}}M'_{-}e^{-ik_{\mathrm{M}z}z}; \tag{57}$$

$$k_{\mathrm{M}z} = \sqrt{k_0^2\varepsilon_{\mathrm{M}} - k_x^2}, \tag{58}$$

where M_{-}, M'_{-} are amplitudes.

At the same time, a semi-infinite PhC mirror at the Brewster's angle is opaque to TE-waves in the bandgap region, and transparent to TM-waves in the entire frequency range. Thus, in the anisotropic microcavity layer only TE-waves can be localized in the bandgap region. If there is a coupling between TE-waves and TM-waves, the TE-wave leaks from the system and manifest itself resonantly in the spectrum of the TM-wave. To find the dispersion equation of the resonance solution, we perform its matching with the solution in the PhC mirror (27). To do this, we find the amplitudes A_{+}, A_{-} of the forward and backward TE-waves of the resonance solution on the left boundary of the A layer adjacent to the anisotropic layer. The TE-wave field in the first layer ($d \le z < d + d_{\mathrm{a}}$) is obtained from eqs. (22) and (23) with $m = 0$:

$$E_{\mathrm{a}y}^{(0)} = A_{+}e^{ik_{\mathrm{a}z}(z-d)} + A_{-}e^{-ik_{\mathrm{a}z}(z-d)}; \tag{59}$$

$$H_{\mathrm{a}x}^{(0)} = \frac{k_{\mathrm{a}z}}{k_0}(-A_+ e^{ik_{\mathrm{a}z}(z-d)} + A_- e^{-ik_{\mathrm{a}z}(z-d)}). \tag{60}$$

The solution for the TM wave in the PhC mirror at the Brewster's angle is a mode propagating without reflection, whose field in the first layer A ($d \le z < d + d_{\mathrm{a}}$) is obtained from eqs. (30) and (31) with $m = 0$ and $A'_- = 0$:

$$E_{\mathrm{a}x}^{(0)} = A'_+ e^{ik_{\mathrm{a}z}(z-d)}; \tag{61}$$

$$H_{\mathrm{a}y}^{(0)} = \frac{k_0 \varepsilon_{\mathrm{a}}}{k_{\mathrm{a}z}} A'_+ e^{ik_{\mathrm{a}z}(z-d)}. \tag{62}$$

Let us match eqs. (54) - (57) and (46) - (53) at the boundary between the metal mirror and the anisotropic layer (for $z = 0$), and eqs. (46) - (53) and eqs. (59) - (62) on the boundary between the anisotropic layer and the PhC mirror (for $z = d$). This gives us, together with (27), the system of 10 equations for 10 unknowns: $M_-, M'_-, E_{\mathrm{e}+}, E_{\mathrm{e}-}, E_{\mathrm{o}+}, E_{\mathrm{o}-}, A_+, A_-, A'_+, K$. This system of equations yields the dispersion equation $\omega(k_x)$.

C. Final equations

The dispersion equation of the resonant TE-mode finally can be written as follows:

$$\frac{x e^{ik_{\mathrm{a}z}d_{\mathrm{a}}} - r_{\mathrm{ab}\perp} e^{-ik_{\mathrm{a}z}d_{\mathrm{a}}}}{x e^{-ik_{\mathrm{b}z}d_{\mathrm{b}}} - r_{\mathrm{ab}\perp} e^{-ik_{\mathrm{b}z}d_{\mathrm{b}}}} - \frac{e^{-ik_{\mathrm{a}z}d_{\mathrm{a}}} - x r_{\mathrm{ab}\perp} e^{ik_{\mathrm{a}z}d_{\mathrm{a}}}}{e^{ik_{\mathrm{b}z}d_{\mathrm{b}}} - x r_{\mathrm{ab}\perp} e^{ik_{\mathrm{b}z}d_{\mathrm{b}}}} = 0. \tag{63}$$

Here

$$x = \frac{\frac{\sin(\phi)}{t_{1\mathrm{ao}}}(r_{1\mathrm{ao}} e^{-ik_{\mathrm{o}z}d} - y e^{ik_{\mathrm{o}z}d}) + \frac{\cos(\phi)}{t_{1\mathrm{ae}}}(U e^{ik_{\mathrm{e}z}d} + V r_{1\mathrm{ae}} e^{-ik_{\mathrm{e}z}d})}{\frac{\sin(\phi)}{t_{1\mathrm{ao}}}(e^{-ik_{\mathrm{o}z}d} - y r_{1\mathrm{ao}} e^{ik_{\mathrm{o}z}d}) + \frac{\cos(\phi)}{t_{1\mathrm{ae}}}(U r_{1\mathrm{ae}} e^{ik_{\mathrm{e}z}d} + V e^{-ik_{\mathrm{e}z}d})}, \tag{64}$$

$$V = \left[\frac{\cos(\phi)}{t_{2\mathrm{ao}}}\left(e^{-ik_{\mathrm{o}z}d} - \left(\frac{t_{1\mathrm{Mo}}(r_{2\mathrm{Mo}} - r_{1\mathrm{Mo}})\cos(\phi)}{t_{1\mathrm{Me}}\alpha_2 \sin(\phi)} + r_{1\mathrm{Mo}}\right) r_{2\mathrm{ao}} e^{ik_{\mathrm{o}z}d}\right) - \frac{\sin(\phi)}{t_{2\mathrm{ae}}}\frac{(r_{2\mathrm{Mo}} - r_{1\mathrm{Mo}})}{\alpha_2} r_{2\mathrm{ae}} e^{ik_{\mathrm{e}z}d}\right] \cdot \left[\frac{\cos^2(\phi)}{t_{2\mathrm{ao}}}\frac{t_{1\mathrm{Mo}}}{t_{1\mathrm{Me}}\sin(\phi)}\left(r_{1\mathrm{Me}} - \frac{\alpha_1}{\alpha_2}\right) r_{2\mathrm{ao}} e^{ik_{\mathrm{o}z}d} + \frac{\sin(\phi)}{t_{2\mathrm{ae}}}\left(e^{-ik_{\mathrm{e}z}d} - \frac{\alpha_1}{\alpha_2} r_{2\mathrm{ae}} e^{ik_{\mathrm{e}z}d}\right)\right]^{-1}, \tag{65}$$

$$U = \frac{-V\alpha_1 + (r_{2\mathrm{Mo}} - r_{1\mathrm{Mo}})}{\alpha_2}, \tag{66}$$

$$y = \frac{t_{1\mathrm{Mo}}\cos(\phi)}{t_{1\mathrm{Me}}\sin(\phi)}(U + V r_{1\mathrm{Me}}) + r_{1\mathrm{Mo}}, \tag{67}$$

$$\alpha_1 = \frac{t_{2\mathrm{Mo}}\sin(\phi)}{t_{2\mathrm{Me}}\cos(\phi)} r_{2\mathrm{Me}} + \frac{t_{1\mathrm{Mo}}\cos(\phi)}{t_{1\mathrm{Me}}\sin(\phi)} r_{1\mathrm{Me}}, \tag{68}$$

$$\alpha_2 = \frac{t_{1\mathrm{Mo}}\cos(\phi)}{t_{1\mathrm{Me}}\sin(\phi)} + \frac{t_{2\mathrm{Mo}}\sin(\phi)}{t_{2\mathrm{Me}}\cos(\phi)}. \tag{69}$$

The Fresnel reflection and transmission coefficients and their analogues are introduced (j = a, M) in Eqs. (70)-(73) :

$$r_{1j\mathrm{e}} = \frac{k_{jz} - k_{\mathrm{e}z}}{k_{jz} + k_{\mathrm{e}z}},\ t_{1j\mathrm{e}} = \frac{2k_{jz}}{k_{jz} + k_{\mathrm{e}z}}; \tag{70}$$

$$r_{1j\mathrm{o}} = \frac{k_{jz} - k_{\mathrm{o}z}}{k_{jz} + k_{\mathrm{o}z}},\ t_{1j\mathrm{o}} = \frac{2k_{jz}}{(k_{jz} + k_{\mathrm{o}z})\cos(\theta_{\mathrm{o}})}; \tag{71}$$

$$r_{2j\mathrm{e}} = \frac{k_{jz}(1 - \frac{\varepsilon_\mathrm{e}}{\varepsilon_\mathrm{o}}\sin^2{(\theta_\mathrm{e})}) - k_{\mathrm{e}z}\cos^2{(\theta_j)}}{k_{jz}(1 - \frac{\varepsilon_\mathrm{e}}{\varepsilon_\mathrm{o}}\sin^2{(\theta_\mathrm{e})}) + k_{\mathrm{e}z}\cos^2{(\theta_j)}},\ t_{2j\mathrm{e}} = \frac{2k_{jz}}{k_{jz}(1 - \frac{\varepsilon_\mathrm{e}}{\varepsilon_\mathrm{o}}\sin^2{(\theta_\mathrm{e})}) + k_{\mathrm{e}z}\cos^2{(\theta_j)}}; \tag{72}$$

$$r_{2j\mathrm{o}} = \frac{k_{jz}\cos^2{(\theta_\mathrm{o})} - k_{\mathrm{o}z}\cos^2{(\theta_j)}}{k_{jz}\cos^2{(\theta_\mathrm{o})} + k_{\mathrm{o}z}\cos^2{(\theta_j)}},\ t_{2j\mathrm{o}} = \frac{2k_{jz}\cos{(\theta_\mathrm{o})}}{k_{jz}\cos^2{(\theta_\mathrm{o})} + k_{\mathrm{o}z}\cos^2{(\theta_j)}}. \tag{73}$$

For certain k_x, the solution of the complex equation (63) is the complex frequency:

$$\omega = \omega_\mathrm{r} - i\gamma, \tag{74}$$

then the spectral position λ_r and the quality factor Q of the resonance are defined:

$$\lambda_\mathrm{r} = 2\pi/\omega_\mathrm{r}, \tag{75}$$

$$Q = \frac{\omega_\mathrm{r}}{2\gamma}. \tag{76}$$

The Q factor of the resonant mode is determined by two components: the material losses of Q_M, to which the absorption of light by the metal layer and the leakage of the TE mode into the continuum of the TM mode $Q(\phi)$ contribute:

$$1/Q = 1/Q_\mathrm{M} + 1/Q(\phi). \tag{77}$$

At $1/Q(\phi) = 0$, the resonant mode becomes the BIC and its real Q factor is limited by material losses in the system. Below we consider two cases leading to the BICs.

D. The symmetry-protected BICs

For rotation angle of the optical axis, the $\phi = 0, \pi/2$, equations (46) - (53) describe a decay into two independent parts for TE- and TM-waves, i.e. the coupling between them disappears. After matching the TE-polarized waves at the interfaces, we obtain an auxiliary dispersion equation for the BICs protected by symmetry, the form of which coincides with (63), but the expression for x changes:

$$x = \frac{r_{\mathrm{a}j\perp}e^{-ik_{jz}d} - r_{\mathrm{M}j\perp}e^{ik_{jz}d}}{e^{-ik_{jz}d} - r_{\mathrm{a}j\perp}r_{\mathrm{M}j\perp}e^{ik_{jz}d}}, \tag{78}$$

where $j = \mathrm{e}$ for $\phi = 0$, and $j = \mathrm{o}$ for $\phi = \pi/2$.

E. The Friedrich-Wintgen BICs

The Friedrich-Wintgen BICs are obtained when the components of the extraordinary and ordinary waves emerging from the anisotropic layer destructively interfere in the continuum. We obtain the auxiliary dispersion equation for the FW BICs by equating to zero the amplitude of A'_+ in (61) - (62) followed by matching the system of equations at the boundaries between the layers:

$$\frac{(ye^{ik_{\mathrm{o}z}d} - e^{-ik_{\mathrm{o}z}d})(Ue^{ik_{\mathrm{e}z}d} - Ve^{-ik_{\mathrm{e}z}d})}{(ye^{ik_{\mathrm{o}z}d} + e^{-ik_{\mathrm{o}z}d})(Ue^{ik_{\mathrm{e}z}d} + Ve^{-ik_{\mathrm{e}z}d})} = \frac{k_{\mathrm{o}z}(1 - \frac{\varepsilon_\mathrm{e}}{\varepsilon_\mathrm{o}}\sin^2{(\theta_\mathrm{e})})}{k_{\mathrm{e}z}\cos^2{(\theta_\mathrm{o})}}. \tag{79}$$

F. The case of the first thicker layer or the layer fabricated of another material

If to extend the first PhC layer by an amount d', then the resonant mode passing through the thickening receives an additional phase shift in the dispersion equation (63). The shift is well described by substitution of x:

$$x' = xe^{2ik_{\mathrm{a}z}d'}. \tag{80}$$

Now assume that the first PhC layer is made of similar material with a thickness d_c. Let the refractive index $n_\mathrm{c} = \sqrt{\varepsilon_\mathrm{c}}$ be close to n_a ($n_\mathrm{c} \approx n_\mathrm{a}$). Then the dispersion equation (63) well describes the resonant mode, if we take into account the additional phase shift in this layer and replace x by:

$$x' = xe^{2ik_{\mathrm{c}z}d'},\ d' = d_\mathrm{c} - k_{\mathrm{a}z}d_\mathrm{a}/k_{\mathrm{c}z},\ k_{\mathrm{c}z} = \sqrt{k_0^2\varepsilon_\mathrm{c} - k_x^2}. \tag{81}$$

G. Case of dielectric structure

In order to describe the structure with two PhC mirrors (Supplementary Figure 3) one can use the method of images [8]. For that we limit a real metal to perfect electric conductor ($n_{\mathrm{M}} \to i\infty$) in Eqs. (70-73). Then the dispersion equation (63) describes the microcavity modes in the structure shown in (Supplementary Figure 3). Another approach with the same dispersion equation is to use the symmetry of the structure. The boundary conditions for $z = d$ do not change. For $z = 0$ we have (for $n_{\mathrm{e}} > n_{\mathrm{M}}$): $E_{ex}(0) + E_{ox}(0) = 0$; $E_{ey}(0) + E_{oy}(0) = 0$. Then the number of equations from the boundary conditions and the number of unknown variables reduces to 8: $(E_{\mathrm{e}+}, E_{\mathrm{e}-}, E_{\mathrm{o}+}, E_{\mathrm{o}-}, A_+, A_-, A'_+, K)$. Supplementary Figure 4 shows the dispersion curves and positions of BICs obtained from Eqs. (63, 78, 79) for ($n_{\mathrm{M}} \to i\infty$). Good agreement with the spectrum numerically calculated for the structure in Supplementary Figure 3 is seen.

In order to understand the mechanism for the occurrence of the FW BICs in more detail, we consider a particular solution (79) in the simple case. Using the method of images ([8]) it can be shown for ideal metal mirror ($n_{\mathrm{M}} = i\infty$) with a normal incidence of light ($\theta_j = 0$) that Eq. (63) describes defect modes with an electric field node in the xy plane in the dielectric structure symmetrically reflected with respect to the xy plane [9]. The condition (79) in this case takes the following form:

$$k_{\mathrm{e}} \tan(k_{\mathrm{o}} d) - k_{\mathrm{o}} \tan(k_{\mathrm{e}} d) = 0, \tag{82}$$

whose solution is given by

$$2d(k_{\mathrm{e}} - k_{\mathrm{o}}) = 2\pi m,\ m \in \mathbb{Z}. \tag{83}$$

Eq. (83) shows that FW BICs occur when an anisotropic defect layer with a thickness $2d$ serves as a full wave phase plate [10]. TE-polarized light incident on such plate preserves original polarization at the plate exit without conversion into the continuum of orthogonal TM-polarization.

SUPPLEMENTARY REFERENCES

[1] Fedorov, F. I. *J. Appl. Spectrosc.* **2**(6), 344–351 (1965).
[2] Yariv, A. and Yeh, P. *Optical waves in crystals. Propagation and control of laser radiation.*, Wiley Inc., New York, NY, USA, (1984).
[3] Shabanov, V. F., Vetrov, S. Y., and Shabanov, A. V. *Optics of Real Photonic Crystals: Liquid Crystal Defects, Irregularities.* [in Russian] SB RAS Publisher, Novosibirsk, Russia, (2005).
[4] Rytov, S. M. *Sov. Phys. JETP* **2**(3), 466–475 (1956).
[5] Shi, H. and Tsai, C.-H. *Solid State Commun.* **52**(12), 953–954 (1984).
[6] Camley, R. E. and Mills, D. L. *Phys. Rev. B* **29**(4), 1695 (1984).
[7] Ignatovich, F. V. and Ignatovich, V. K. *Usp. Fiz. Nauk* **182**(7), 759 (2012).
[8] Landau, L. D., Lifshitz E. M. *Electrodynamics of continuous media.* Pergamon, Oxford, UK (1984).
[9] Timofeev, I. V., Maksimov, D. N., and Sadreev, A. F. *Phys. Rev. B* **97**(2), 24306 (2018).
[10] Azzam, R. M. A. and Bashara, N. M. *Ellipsometry and polarized light.* North-Holland Pub. Co., Amsterdam, Netherlands, (1977).